Classical and Mixed Quantum Mechanical/Molecular Mechanical Simulation of Hydrated Manganous Ion

Jorge Iglesias Yagüe, Ahmed M. Mohammed,† Hannes Loeffler, and Bernd M. Rode*

Department of Theoretical Chemistry, Institute of General, Inorganic and Theoretical Chemistry, University of Innsbruck, A-6020 Innsbruck, Austria

Received: February 5, 2001; In Final Form: May 22, 2001

An ab intio two-body analytical potential function was constructed to describe Mn(II)−water interactions. Classical Monte Carlo (MC) and molecular dynamics (MD) simulations have been performed to study the hydration structure of Mn(II). The study was extended to a combined QM/MM-MD level in order to investigate the influence of higher (*n*-body) terms. The structure of the hydrated ion is discussed in terms of radial distribution functions, coordination numbers, and angular distributions. The results of the QM/MM-MD simulations have been found to be much closer to the experimental values, proving that many-body effects play an important role in the description of the hydrated Mn(II) ion.

1. Introduction

The study of metal ion hydration is quite important not only for the understanding of the thermodynamic and kinetic behavior of metals ions[1−3] but also for the interpretation of the structure and function of many biomolecules in which metal ion interactions play a role.[4,5] Hence, investigations have been carried out to determine the structure and dynamics of metal ions in solution by a variety of spectroscopic techniques such as nuclear magnetic resonance (NMR), extended X-ray absorption fine structure spectroscopy (EXAFS), Mössbauer, infrared (IR), and Raman spectroscopy,[6−8] and scattering techniques such as X-ray, electron and neutron diffraction,[6,9,10] and electrochemical techniques[11,12] and by theoretical methods, mostly simulations of the Monte Carlo (MC), molecular dynamics (MD), and quantum mechanics/molecular mechanics (QM/MM) types.[6,13−18]

In theoretical studies, classical MC/MD simulation techniques have been used widely for the study of solvation structure of metal ions. The QM/MM approach has also been used successfully, within the Molecular Dynamics and Monte Carlo scheme to study ionic solvation.[19−24] However, the types of metal under study and ion−solvent interaction potentials used have affected their degree of success. In some monovalent and divalent metal ions with only pairwise additive intermolecular potentials, structural results that are in good agreement with those obtained experimentally have been achieved.[25−29] Nevertheless, in most cases, with divalent and trivalent metals, the inclusion of many-body interactions has been shown to be crucial.[13,14,30−32] The failure of pairwise addivity for cation−water potentials, particularly for divalent and trivalent ions, has been handled in various ways. One approach that has been used is the nearest-neighbor ligand correction (NNLC)[33a,b] algorithm, which uses in addition to pair potential terms a three-body correction term based on ab initio calculations of the molecular interaction energy surface of the metal ion monohydrate with another water molecule. However, the most successful and exact approach is to supplement the potential energy function to be employed by many-body terms. In many cases, three-body potentials calculated by ab initio methods have reproduced properly hydration numbers.[30,31]

The solvation structure of Mn(II) has been studied to a lesser extent, both experimentally and theoretically, than that of other divalent first-row transition metal ions such as Fe^{2+}, Cu^{2+}, Ni^{2+}, and Zn^{2+}, but interest has increased recently since its importance in several biological systems has been recognized.[34a,b] In many solvents, including water, the solvation structure of the Mn(II) ion has been determined to be a six-coordinated octahedral using X-ray (XD),[6,10] neutron diffraction[35] (ND), and EXAFS.[6,36] In contrast to the relatively large number of experimental studies[6,10,35,36] on hydration structure of Mn(II), only few preliminary theoretical studies are reported.[37,38]

In the present study, a two-body analytical potential function was constructed, a combined QM/MM formalism has been implemented in a MD simulation program, and MC, MD, and QM/MM-MD simulations were carried out with an optimized pair potential for Mn(II) in water.

2. Computational Details

2.1. Computer Resources and Parallelization. Classical MC and MD simulations were performed on single-processor machines, leading to a total computational time of 2 days for MC (3 million configurations for equilibration and 3 million for sampling) on a MIPS R8000 machine and 11 h for MD (60 000 time steps for equilibration and 300 000 for sampling) on an Intel Pentium II 500 MHz. In contrast, the large time consumption of the QM/MM-MD simulation requires the use of special hardware configuration. A cluster of 9 dual Intel Pentium III 550 MHz processor machines using a standard 100 Mbs ethernet link was employed for this method. The configuration of the cluster machine and the use of the TURBOMOLE[39a−d] package allow parallelization of the computations and hence reduce considerably the computer time required. We have studied the possible degree of parallelization of the simulation, varying the number of processors. The results show that the use of six processors gives the optimal usage of resources (Table 1). Most of the gain in computer time refers to the quantum chemical calculations, which contribute as 95%

* Corresponding author.
† Permanent address: Department of Chemistry, Addis Ababa University, P.O. Box 1176, Addis Ababa, Ethiopia.

10.1021/jp010436g CCC: $20.00
Published on Web 07/21/2001

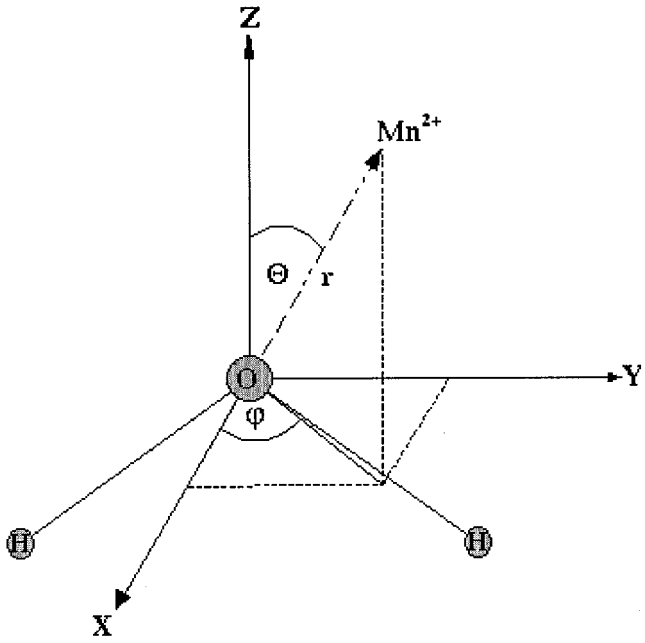

Figure 1. Definition of geometric variables for Mn(II)−water orientations. H_2O molecules in *yz* plane.

TABLE 1: Relative Speeds on a TURBOMOLE Calculation Using Different Number of Processors

number of processors	relative speed
1	1
2	1.9
4	3.3
6	3.7

to the total computer time. With respect to this fact, any change of the classical MD/MC programs to a more parallelized code would not have any substantial effect on the overall CPU time needed. Using the 6-processors cluster, the computation of 42000 time steps in the QM/MM-MD simulation needed a total of 151 days of CPU time.

2.2. Construction of Ion−Water Pair Potential. To construct the Mn(II)−H_2O pair potential, we placed the Mn(II) ion at numerous positions around the water molecule by varying geometrical parameters $0° \leq \Theta \leq 180°$ and $0° \leq \varphi \leq 90°$; for each configuration, the Mn−O internuclear distance *r* was varied from 1.2 to 15.0 Å (Figure 1). The internal geometric parameters of water were held fixed at the experimental values,[40] i.e., $r_{OH} = 0.957$ Å and $\angle HOH = 104.5°$. The quantum chemical calculations were performed at the UHF level using the TURBOMOLE program. The ab initio effective core potentials (ECP) and double-ζ valence basis set developed by Stevens, Krauss, and Basch[41] were used for the Mn(II) ion, and for oxygen and hydrogen atoms, the DZP basis sets of Dunning were used.[42]

The interaction energies, ΔE_{2bd}, between water and manganous ion were evaluated by subtracting the ab initio energies of the isolated species $E_{Mn^{2+}}$ and E_{H_2O} from those of the monohydrates $E_{Mn(H_2O)^{2+}}$

$$\Delta E_{2bd} = E_{Mn(H_2O)^{2+}} - E_{Mn^{2+}} - E_{H_2O} \quad (1)$$

A total of 1782 energy points of the monohydrate was generated for a representative description of the Mn(II)−H_2O system. Then fitting was performed with various potential types to describe electrostatic and van der Waals interactions.

2.3. Monte Carlo Simulation. MC simulation was carried out in the canonical ensemble using the Metropolis[43] algorithm. The optimized pair potential function was applied to a system consisting of one Mn(II) ion and 199 water molecules in a periodic cube at a temperature of 298.16 K. A spherical cutoff at half of the box length (9.117 Å) was introduced. The density of 0.997 g cm^{-3} was assumed to be the same as that of pure water. For water−water interactions, the CF2 potential[44] was used, as this model is more consistent than the MCY[45] model with our type of ion−water potential.[46] After generating a starting configuration randomly, the system reached energetic equilibrium after 3 million configurations. For evaluation of structural data, especially the radial distribution functions (RDFs), a further 3 million configurations were sampled.

2.4. Molecular Dynamics Simulation. Consistent with the MC simulation, the same pair potential and the same box characteristics were applied. Correspondingly, a radial cutoff limit of half the box length (i.e., 9.117 Å) for Coulombic and non-Coulombic terms was chosen with the exception of non-Coulombic O−H and H−H interactions,where a cutoff of 5 and 3 Å, respectively, was sufficient. In addition, a reaction field[47] was established to properly account for long-term Coulombic interactions.

Since the CF2[48a,b] water model used in this simulation allows explicit hydrogen movement, the time step was chosen to be 0.2 fs. The water box, subject to periodic boundary conditions, was equilibrated for 12.0 ps (60000 time steps) in the NVT ensemble. To maintain a constant temperature of 298.16 K, we applied a temperature scaling algorithm[49] with a relaxation time of $\tau = 0.1$ ps along the whole simulation. A further 300 000 steps of MD simulation resulting in a total simulation time of 60.0 ps were carried out under the same condition as that of the equilibration to provide data for structural evaluation.

2.5. Quantum Mechanics/Molecular Mechanics Simulation. A hybrid QM/MM-MD simulation was performed, describing the crucial first hydration shell at the UHF level in order to properly account for many-body effects. The quantum mechanical region around the metal ion had a radius of 4.0 Å, and water molecules were allowed to leave and enter from and to this zone dynamically. The size of this region was chosen to contain the full first hydration shell at any step of the simulation. A smoothing function in the radial region between 3.8 and 4.0 Å had to be applied to ensure a smooth transition between the QM and MM forces.[17] In each simulation step, an ab initio calculation was performed providing quantum mechanical forces to be incorporated into the total force of the system by the following formula

$$F_{System,total} = F_{System,MM} + F_{QM-Region,QM} - F_{QM-Region,MM} \quad (2)$$

where $F_{System,total}$ is the total force of the system, $F_{System,MM}$ is the MM force of the system, $F_{QM-Region,QM}$ is the QM force in the QM region, and $F_{QM-Region,MM}$ is the MM force in the QM region. The last term in eq 2 accounts for the coupling between QM and MM region.

The parallelized TURBOMOLE package was used for the calculation of the ab initio forces, with the same basis sets[41,42] for Mn(II), O, and H as those in the calculation of the pair potential.

The simulation protocol was the same as that in the classical MD simulation. The starting configuration of the system was taken from the last configuration of the pair potential simulation. The system was reequilibrated for 4.2 ps (21000 time steps) in the NTV-ensemble. A further 21 000 steps of QM/MM-MD simulation (4.2 ps) were performed in order to obtain data for structural evaluation.

TABLE 2: Final Optimized Parameters for the Interactions of O and H Atoms of Water with Mn^{2+} Together with the Point Charges Applied for the Interaction between Mn^{2+} and H_2O

		a	b	c	d
		Å^{-5}	Å^{-7}	Å^{-9}	Å^{-12}
atom	charge (a.u.)[a]	(kcal/mol)	(kcal/mol)	(kcal/mol)	(kcal/mol)
O	−0.6598	−7711.56	47036.41	−81898.47	66161.08
H	0.3299	−706.76	7575.35	−18087.79	18731.51

[a] Taken from the CF2[43] water−water interaction potential.

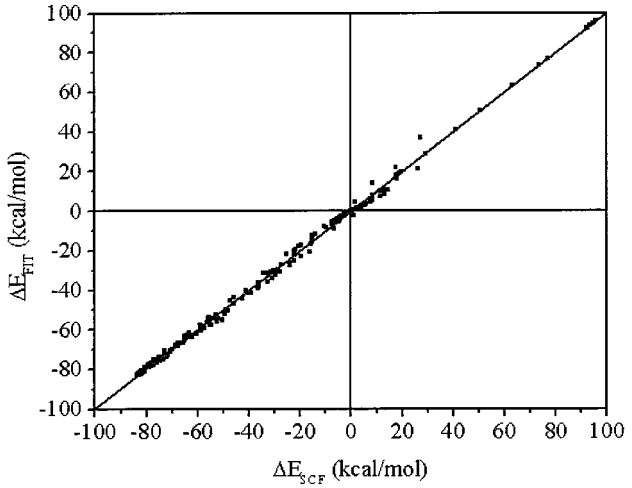

Figure 2. Comparison of the stabilization energies obtained from ab initio calculations (ΔE_{SCF}) and the fitted energies (ΔE_{FIT}).

3. Results and Discussion

3.1. Pair Potential. A global minimum of −74.17 kcal/mol was found for the dipole-oriented C_{2v} configuration of the $Mn^{2+}-H_2O$ system at a Mn−O distance of 2.05 Å ($\Theta = 0$ and $\varphi = 0$, Figure 1).

The fitting, performed by the least-squares method of Levenberg-Marquart resulted in a function of the form

$$\Delta E_{FIT} = \sum_i (a_{iM} r_{iM}^{-5} + b_{iM} r_{iM}^{-7} + c_{iM} r_{iM}^{-9} + d_{iM} r_{iM}^{-12} + q_i q_M r_{iM}^{-1}) \quad (3)$$

where a_{iM}, b_{iM}, c_{iM}, and d_{iM} are fitting parameters, r_{iM}'s are the distances between the ith atom of H_2O and Mn(II), q_i's are the atomic net charges of the ith atom of H_2O, and q_M is the atomic net charge of Mn(II). A weight factor was introduced to give special emphasis to values near the global energy minimum. Values above 30 kcal/mol were excluded. Similar analytical potential functions were reported for other hydrated metal ions.[30,31] The fitting resulted in a rms error of 1.70. The final parameters of the function are given in Table 2.

In Figure 2, the stabilization energies obtained from the quantum chemical calculations, ΔE_{SCF} (eq 1), are plotted versus those obtained from the analytical function ΔE_{FIT}, (eq 3) The correlation between the energies ΔE_{SCF} and ΔE_{FIT} is an important parameter, which indicates the quality of the function. To show this correlation, we graph potential curves for some characteristic geometrical arrangements in Figure 3. They show satisfactory agreement even in the repulsive regions.

3.2. Structural Data. Figure 4 displays and compares the radial distribution functions (RDFs) for Mn(II)−O and Mn-(II)−H together with their corresponding running integration numbers obtained from MC, MD, and QM/MM-MD simulations. Their characteristic values are listed in Table 3. In the Mn(II)−O RDFs, the peaks corresponding to the first hydration shell are centered at 2.23 Å for the MC, 2.22 Å for the MD, and 2.28 Å for the QM/MM-MD simulations, 0.18, 0.17, and 0.22 Å beyond the minimum of the SCF Mn(II)−H_2O potential, respectively. The values obtained do not differ much from the experimental values ranging from 2.18 to 2.22 Å.[6]

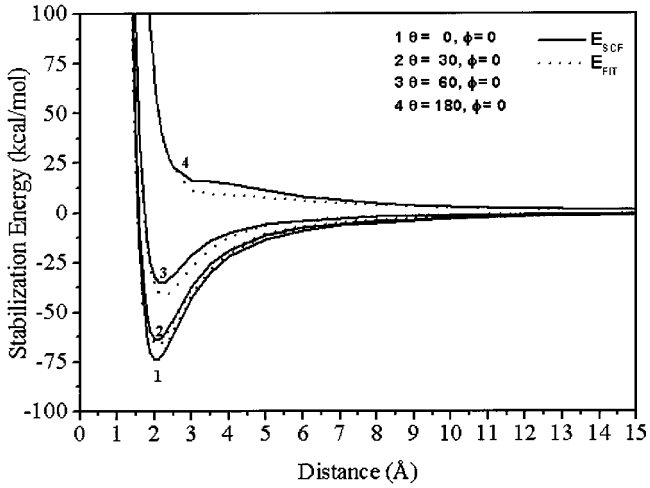

Figure 3. Comparison of ΔE_{SCF} and ΔE_{FIT}, using the final parameters for values of $\theta = 0°$, 60°, 90°, and 180° ($\phi = 0$ in all cases).

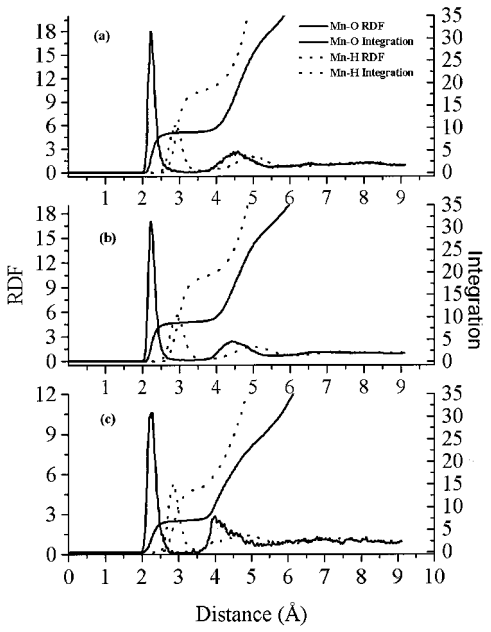

Figure 4. Mn−O and Mn−H radial distribution functions and their running integration number for Mn(II)−water system obtained by (a) MC, (b) MD, and (c) QM/MM-MD.

TABLE 3: Characteristic Values of the Radial Distribution Functions, $g_{\alpha\beta}(r)$, for the Mn(II)−Water Solution Obtained from MC, MD, and QM/MM-MD Simulations

method	α−β	r_{M1}	r_{m1}	n_1	r_{M2}	r_{m2}	n_2
MC	Mn−O	2.23	2.94	8.90	4.59	5.53	22.83
	Mn−H	2.92	3.53	17.04	4.82	6.07	53.44
MD	Mn−O	2.22	3.26	8.74	4.42	5.62	22.74
	MnH	2.94	3.76	19.11	4.98	6.16	53.13
QM/MM	Mn−O	2.28	2.88	6.74	4.00	5.20	18.06
	Mn−H	2.84	3.44	13.67	4.80	5.94	48.00

[a] r_{Mi} and r_{Mi} are the distances in Å for the ith maxima and minima of $g_{\alpha\beta}(r)$, respectively, n_j is the average coordination number integrated up to r_{Mi} of the ith shell.

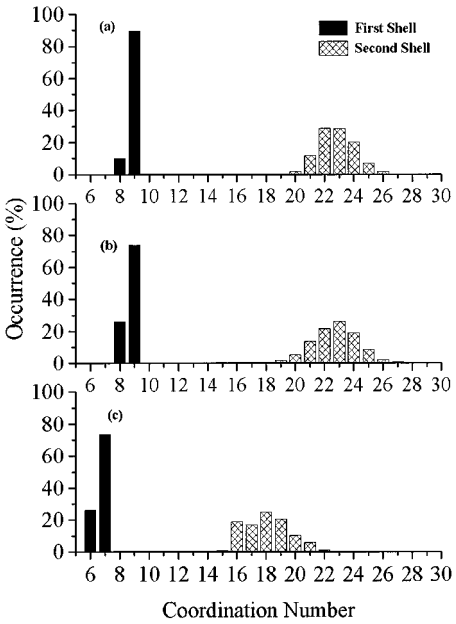

Figure 5. First- and second-shell coordination number distribution of hydrated Mn(II) for the (a) MC, (b) MD, and (c) QM/MM-MD simulations.

The second peaks in these functions related to the second hydration shell appear between 3.80 and 5.34 Å with a maximum value at 4.59 Å for the MC, between 3.72 and 5.32 Å with a maximum value at 4.42 Å for the MD, and between 3.72 and 5.20 Å with maximum value at 4.42 Å for the QM/MM-MD, clearly well separated from the first hydration sphere in all simulations.

In the Mn(II)−H RDFs, the first peaks are centered at 2.92, 2.94, and 2.84 Å for the MC, MD, and QM/MM-MD simulations, respectively. The shift of the Mn−H RDFs to larger distances with respect to the corresponding oxygen peaks indicates that especially in the first shell, the water molecules are well oriented to obey the dominant ion−water interactions, with their oxygen atoms pointing to the ion.

The percentages of occurrence of coordination numbers in the first and second shells as obtained from the running integration numbers are shown in Figure 5. For the MC simulation, coordination numbers of 10.33% of 8 and 89.67% of 9 with a mean value of 8.90 water molecules and, for the MD simulation, 26% of 8, 73.73% of 9 and 0.27% of 10 water molecules with mean value of 8.74 water molecules were observed. However, for the QM/MM-MD simulation, 26.42% of 6 and 73.57% of 7 water molecules around the cation with a mean value of 6.74 water molecules were obtained, i.e., about 2 water molecules less than the averages obtained from the classical MC/MD simulations.

The mean coordination numbers for the second hydration shell are 22.83, 22.74, and 18.06 for MC, MD, and QM/MM-MD simulations, respectively, implying that every first shell water molecule interacts with about 2.6 water molecules in the second shell in all simulations.

The uneven second shell coordination number distribution obtained by the QM/MM-MD method rather indicates that more steps are needed in order to obtain a smooth equilibrium distribution.

The $H_2O-Mn-H_2O$ angular distributions are shown in Figure 6. The angular distributions obtained for the MC and MD simulations are almost the same except for the small third peak observed at 120° for the MD simulation. The first peak

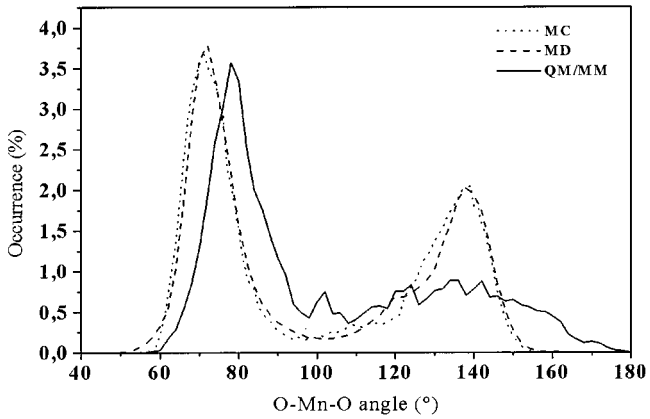

Figure 6. Distribution of the bond angles $H_2O-Mn(II)-H_2O$ for the (a) MC, (b) MD, and (c) QM/MM-MD simulations.

describing the most direct neighbors appears between 59° and 93° centered at 71° for MC and between 50° and 98° centered at 72° for the MD simulation. The second peaks are centered at 139° and 138° for the MC and MD simulations, respectively. No angle larger than 160° appeared in these distributions. In contrast to the angular distributions obtained from classical MC/MD simulations, the one obtained from the QM/MM-MD simulation ranges from 59° to 179°. The first peak is centered at 78° and the second at 136°. The first peak is centered, therefore, at an angle larger by 6° and 7° than the first peaks obtained by classical simulations. This is to be attributed to the smaller number of water ligands in the first hydration shell as compared to the number of molecules in the case of MC/MD simulations.

4. Conclusion

The ab initio two-body potential is not adequate to describe the hydration structure of Mn(II) and leads to an overestimation of the coordination number, even using the more powerful QM/MM-MD method. The differences between the classical and the QM/MM-MD studies prove that many-body effects play an important role in the description of the hydration structure of Mn(II). The results of the QM/MM-MD methodology are much closer to the experimental values. Despite the accuracy of the QM/MM-MD study, its results still raise the question for a need of *n*-body correction terms outside the QM region. The box-size effect could also have an effect on the results obtained for the second hydration shell, due to the possibility of significant interactions with a third solvation shell. For these reasons, a further extension of the present study employing a 3-body correction function for the MM region and an extended basic box seems to be desirable.

Acknowledgment. Financial support by The Austrian Science Foundation, project No. P13644-TPH, and a scholarship of the Austrian Federal Ministry for Foreign Affairs for A.M.M. are gratefully acknowledged.

References and Notes

(1) Marcus, Y. *Ion Solvation*; John Wiley & Sons Ltd.: Chichester, U.K., 1986; Chapters 4 and 6.

(2) Burger, K. *Solvation, Ionic and Complex Formation Reactions in Non-Aqueous Solvents;* Elsevier: Amsterdam, 1983; Chapter 6.

(3) Burgess, J. *Metal ions in Solution;* John Wiley & Sons Ltd.: Chichester, U.K., 1978.

(4) Creighton, T. E. *Proteins: Structure and Molecular Properties,* 2nd ed.; W. H. Freeman & Co.: New York, 1993.

(5) Babu, Y. S.; Sack, J. S.; Greenough, T. J.; Bugg, C. E.; Means, A. R.; Cook, W. J. *Nature* **1985**, *315*, 37.

(6) Ohtaki, H.; Radnai, T. *Chem. Rev.* **1993**, *93*, 1157.
(7) Enderby, J. E.; Neilson, G. W. *Rep. Prog. Phys.* **1981**, *44*, 593.
(8) Aizawa, S.; Matsuda, K.; Tajima, T.; Maeda, M.; Sugata, T.; Funahashi, S. *Inorg. Chem.* **1995**, *34*, 2042.
(9) Ozutsumi, K.; Koide, M.; Suzuki, H.; Ishiguro, S. *J. Phys. Chem.* **1993**, *97*, 500.
(10) Cotton, F. A.; Daniels, L. M.; Murillo, C. A.; Quesada, J. F. *Inorg. Chem.* **1993**, *32*, 4861.
(11) Conway, B. E. *Ionic Hydration in Chemistry and Physics*; Elsevier: Amsterdam, 1981.
(12) Amis, E. S.; Hinton, J. F. *Solvent Effects on Chemical Phenomena*; Academic: New York, 1973.
(13) Pranowo, H. D.; Rode, B. M. *J. Phys. Chem. A* **1999**, *103*, 4298.
(14) Marini, G. W.; Liedl, K. R.; Rode, B. M. *J. Phys. Chem. A* **1999**, *103*, 11387.
(15) Kowall, T.; Foglia, F.; Helm, L.; Merbach, A. E. *J. Am. Chem. Soc.* **1995**, *117*, 3790.
(16) Marx, D.; Sprik, M.; Parrinello, M. *Chem. Phys. Lett.* **1997**, *273*, 360.
(17) Kerdcharoen, T.; Liedl, K. R.; Rode, B. M. *Chem. Phys.* **1996**, *211*, 313.
(18) Martínez, J. M.; Cobos, J. H.; Martin, H. S.; Pappalardo, R. R.; Blake, I. O.; Sánchez Marcos, E. *J. Chem. Phys.* **2000**, *112*, 2339.
(19) Kerdcharoen, T.; Rode, B. M. *J. Phys. Chem. A* **2000**, *104*, 7073.
(20) Gao, J. In *Review of Computational Chemistry*; Lipkowitz, K. B., Boyd, D. B., Eds.; VCH: New York, 1996; Vol. 7, p 119.
(21) Tongraar, A.; Rode, B. M. *J. Phys. Chem. A* **1999**, *103*, 8524.
(22) Tongraar, A.; Liedl, K. R.; Rode, B. M. *J. Phys. Chem. A* **1998**, *102*, 10340.
(23) Tongraar, A.; Liedl, K. R.; Rode, B. M. *Chem. Phys. Lett.* **1998**, *286*, 56.
(24) Tongraar, A.; Liedl, K. R.; Rode, B. M. *J. Phys. Chem. A* **1997**, *101*, 6299.
(25) Limtrakul, J. P.; Probst, M. M.; Rode, B. M. *J. Mol. Struct. (THEOCHEM)* **1985**, *23*, 121.
(26) Bopp, P.; Okada, I.; Ohtaki, H.; Henizinger, K. *Z. Naturforsch., Teil A* **1985**, *40*, 116.
(27) Spohr, E.; Pálinkás, G.; Heinzinger, K.; Bopp, P.; Probst, M. M. *J. Phys. Chem.* **1988**, *92*, 6754.
(28) Pranowo, H. D.; Bambang Setiaji, A. H.; Rode, B. M. *J. Phys. Chem. A* **1999**, *103*, 11115.
(29) Curtiss, L. A.; Jurgens, R. *J. Phys. Chem.* **1990**, *94*, 5509.
(30) Marini, G. W.; Texler, N. R.; Rode, B. M. *J. Phys. Chem.* **1996**, *100*, 6808.
(31) Texler, N. R.; Rode, B. M. *J Chem. Phys.* **1995**, *99*, 15714.
(32) Cordeiro, M. N. D. S.; Gomes, J. A. N. F.; González-Lafont, A.; Lluch, J. M.; Bertrán, J. *Chem. Phys.* **1990**, *141*, 379.
(33) (a) Rode, B. M.; Islam, S. M. *Z. Naturforsch., Teil A* **1991**, *46*, 357. (b) Yongyai, Y.; Kokpol, S.; Rode, B. M. *Chem. Phys.* **1991**, *156*, 403.
(34) (a) Lawrance, G. D.; Sawyer, D. T. *Coord. Chem. Rev.* **1978**, *27*, 173. (b) Chiswell, B.; Mckenzie, D.; Lindoy, L. F. In *Comprehensive Coordination Chemistry*; Wilkinson, G., Gillard, R. D., McCleverty, A. M., Eds.; Pergamon Books Ltd.: Elmsford, NJ, 1987; pp 1−122.
(35) Neilson, G. W.; Newsome, J. R.; Sandstorm, M. *J. Chem. Soc., Faraday Trans. 2* **1981**, *17*, 1245.
(36) Ozutsumi, K.; Koide, M.; Suzuki, H.; Ishiguro, S. *J. Phys. Chem.* **1993**, *97*, 500.
(37) Babu, C. S.; Lim C. *J. Phys. Chem. B* **1999**, *103*, 7958.
(38) Sivaraja, M.; Stouch, T. R.; Dismukes, G. C. *J. Am. Chem. Soc.* **1992**, *114*, 9600.
(39) (a) Ahlrichs, R.; Bär, M.; Häser, M.; Horn, H.; Kölmel, C. *Chem. Phys. Lett.* **1989**, *162*, 165. (b) Brode, S.; Horn, H.; Ehrig, M.; Moldrup, D.; Rice, J. E.; Ahlrichs, R. *J. Comput. Chem.* **1993**, *14*, 1142. (c) von Arnim, M.; Ahlrichs, R. *J. Comput. Chem.* **1998**, *19*, 1746. (d) Ahlrichs, R:, von Arnim, M. In *Methods and Techniques in Computational Chemistry: METECC-95*; Clementi, E., Corongiu, G., Eds.; Club Européen MOTECC: Namur, Belgium, 1995; pp 509−554.
(40) Benedict, W. S.; Gailar, N.; Plyler, E. K. *J. Chem. Phys.* **1956**, *24*, 1139.
(41) Stevens, W. J.; Krauss, M.; Basch, H.; Jasien, P. G. *Can. J. Chem.* **1992**, *70*, 612.
(42) Dunning, T. H., Jr. *J Chem. Phys.* **1970**, *53*, 2823.
(43) Metropolis, N.; Rosenbluth, A. W.; Teller, A. H.; Teller, E. *J. Chem. Phys.* **1953**, *21*, 1087.
(44) Jancsó, G.; Heinzinger, K.; Bopp. P. *Z. Naturforsch.* **1985**, *A40*, 1235.
(45) Matsuoka, O.; Clementi, E.; Yoshimine, M. *J. Phys. Chem.* **1976**, *79*, 1351.
(46) Rode, B. M. *J. Phys. Chem.* **1992**, *96*, 4170.
(47) Müller-Plathe, F. *Comput. Phys. Commun.* **1993**, *78*, 77.
(48) (a) Stillinger, F. H.; Rahman, A. *J. Chem. Phys.* **1978**, *68*, 666. (b) Janscó, G.; Bopp, P.; Heinzinger, K. *Chem. Phys. Lett.* **1983**, *98*, 129.
(49) Berendsen, H. J. C.; Postma, J. P. M.; van Gunsteren, W. F.; DiNola, A.; Haak, J. R. *J. Chem. Phys.* **1984**, *81*, 3685.